The EMBO Journal (2007) 26, 265–274 | © 2007 European Molecular Biology Organization | All Rights Reserved 0261-4189/07
www.embojournal.org

THE EMBO JOURNAL

Reversible movement of switch 1 loop of myosin determines actin interaction

Bálint Kintses[1], Máté Gyimesi[1], David S Pearson[2], Michael A Geeves[2], Wei Zeng[3], Clive R Bagshaw[3] and András Málnási-Csizmadia[1,*]

[1]Department of Biochemistry, Eötvös Lorand University, Budapest, Hungary, [2]Department of Biosciences, University of Kent, Canterbury, Kent, UK and [3]Department of Biochemistry, University of Leicester, Leicester, UK

The conserved switch 1 loop of P-loop NTPases is implicated as a central element that transmits information between the nucleotide-binding pocket and the binding site of the partner proteins. Recent structural studies have identified two states of switch 1 in G-proteins and myosin, but their role in the transduction mechanism has yet to be clarified. Single tryptophan residues were introduced into the switch 1 region of myosin II motor domain and studied by rapid reaction methods. We found that in the presence of MgADP, two states of switch 1 exist in dynamic equilibrium. Actin binding shifts the equilibrium towards one of the MgADP states, whereas ATP strongly favors the other. In the light of electron cryo-microscopic and X-ray crystallographic results, these findings lead to a specific structural model in which the equilibrium constant between the two states of switch 1 is coupled to the strength of the actin–myosin interaction. This has implications for the enzymatic mechanism of G-proteins and possibly P-loop NTPases in general.

The EMBO Journal (2007) **26,** 265–274.
doi:10.1038/sj.emboj.7601482
Subject Categories: structural biology
Keywords: actomyosin interaction; G-proteins; Mg-binding; nucleotide binding; tryptophan fluorescence

Introduction

The family of P-loop proteins, which includes G-proteins and the motor proteins myosin and kinesin, is able to sense the difference between NTP and NDP bound in the nucleotide pocket through the P-loop itself and two additional loops known as switch 1 and 2. The conformation of the loops can then influence the interactions with partner proteins, particularly the exchange factors (GEFs in G-proteins or the track proteins actin and tubulin for motor proteins). The switch 1 loop is thought to be the region primarily responsible for the communication between the nucleotide-binding pocket and the binding region of the nucleotide exchange factor (Boriack-Sjodin *et al*, 1998; Holmes *et al*, 2003; Naber *et al*, 2003). How switch 1 can transmit information about the type of nucleotide (NTP or NDP) towards the partner binding region and regulate the binding strength of the partner protein remains to be understood. As actin binding to myosin strongly depends on whether ADP or ATP is in the nucleotide - binding pocket, this system is very suitable to study the role of switch 1 in this mechanism.

Myosins are ATP-driven molecular motors that generate force and move along actin filaments. During the ATPase cycle of myosin, its binding strength with actin changes cyclically. Nucleotide and actin binding are generally antagonistic, although the actual dissociation constant for actomyosin depends on the type of the nucleotide bound to myosin and the myosin isoform. In the case of myosin II, actin and myosin interact weakly in the presence of ATP, but more strongly in the presence of ADP.

Recently, Holmes *et al* (2003) showed that the actin-binding cleft of myosin II is closed in the rigor state and cleft closure is induced by the actin-binding process (Conibear *et al*, 2003). The recent apo atomic structures of myosin II and V suggested that switch 1 opening is accompanied by closure of the actin-binding cleft to give the strongly actin-bound form of myosin (Coureux *et al*, 2003; Reubold *et al*, 2003). The ADP-bound state is regarded as a strong actin-bound form, although two different conformations of the switch 1 loop were found (Supplementary Figure S1) (Gulick *et al*, 1997; Coureux *et al*, 2004). Nevertheless, switch 1 movements have not been investigated directly and several questions arise: (1) If two ADP states of switch 1 exist, what is the equilibrium constant between them? (2) How is the putative equilibrium of two states of switch 1 affected by different nucleotides and by Mg^{2+}? (3) What is the relationship between actin and nucleotide binding to myosin and switch 1 movement? (4) What is the role of this equilibrium in the chemo-mechanical cycle of myosin?

To answer these questions we introduced single tryptophan residues into the switch 1 region of the *Dictyostelium discoideum (Dd)* myosin II motor domain as fluorescence probes to follow conformational transitions. Tryptophan residues were engineered into position F239 (M_{W239+}) or F242 (M_{W242+}), which are conservative substitutions to minimize structural perturbation by the mutations (Figure 1). F239 is the neighboring amino acid of the R238–E459 salt bridge, which connects switch 1 to switch 2 loop, and therefore this fluorophore is likely to sense conformational changes related to the structural coupling of these loops. F242 is located along the β-strand that extends from the switch 1 loop. Here, we show that M_{W239+} and M_{W242+} mutants respond to nucleotide and actin binding with large fluorescence changes. Based on transient kinetic experiments on these mutants, we conclude that the actin-binding cleft movement is kinetically coupled with the movement of switch 1 but they do not move together as a rigid body. We confirm structural data that indicates that switch 1 exists in two states in the presence of MgADP and find that there is a dynamic equilibrium between

*Corresponding author. Department of Biochemistry, Eötvös Lorand University, Budapest 1117, Hungary. Tel.: +36 1 381 2171; Fax: +36 1 381 2172; E-mail: malna@elte.hu

Received: 18 April 2006; accepted: 25 October 2006

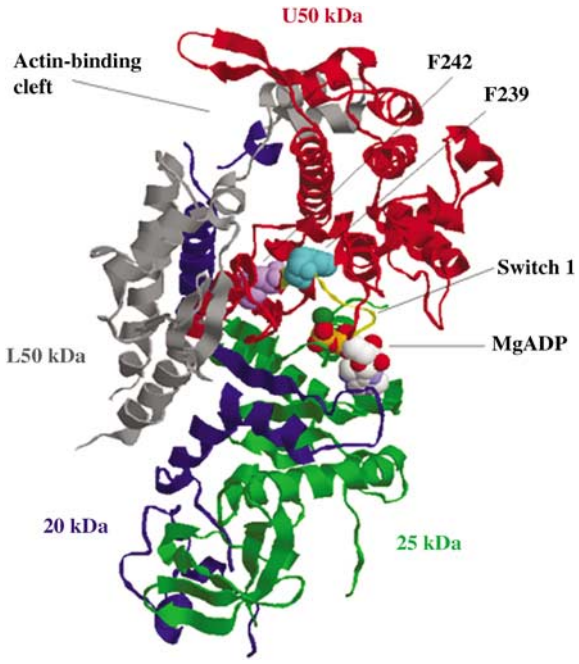

Figure 1 Ribbon model of MgADP complex of *Dd* myosin II motor domain (1MMA). F239 (cyan) and F242 (purple) and MgADP are highlighted by spacefill modeling. Subdomains are color-labeled: N-terminal (25 kDa) subdomain is shown in green, lower 50-kDa subdomain in gray, upper 50-kDa subdomain in red, C-terminal (20 kDa) subdomain in blue. The switch 1 loop (yellow) comprises residues 233–240.

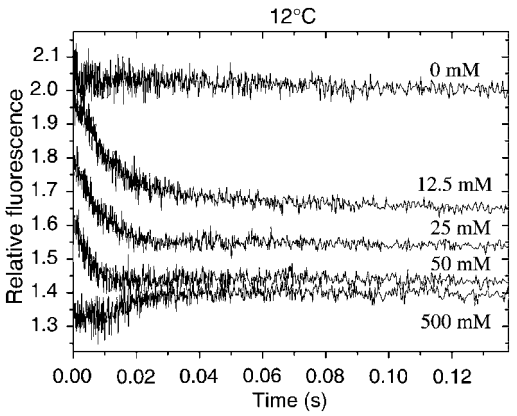

Figure 2 Time course of the fluorescence intensity signals for the reaction of 2 μM M_{W239+} with 0, 12.5, 25, 50 and 500 μM of MgADP in stopped flow at 12°C. The dead time of the stopped-flow measurements was 1.5 ms. The ligand binding phase appeared as a quench phase. As the amplitude loss becomes very significant at higher ADP concentrations, the maximum rate constant of ligand binding is uncertain, but is estimated to be between 1000 and 1500 s^{-1}. At high ADP concentration, a fluorescence enhancement can be distinguished from the quenching phase. The fluorescence enhancement represents the equilibration of the two ADP states with an observed rate constant of 55 s^{-1} at 12°C.

them. This equilibrium is pushed by ATP and actin to the switch 1 closed and open states, respectively. Based on these effects, we construct a model that explains the different actin affinities of ATP and ADP complexes of myosin.

Results

Steady-state fluorescence of M_{W239+} and M_{W242+} in the presence of different nucleotides

We monitored the effect of different nucleotides on the fluorescence emission spectra of M_{W239+} and M_{W242+}. Nucleotides caused a large fluorescence quench in both constructs. All of the nucleotides and nucleotide analogs in the presence and absence of Mg^{2+} had the same effect on M_{W242+} fluorescence, an approximately 20% quench. In contrast, with the M_{W239+} construct at 20°C, MgATP induced a 37% quench and 10 nm blue shift, whereas MgADP gave a 20% quench and 3 nm blue shift (Supplementary Figure S2). All of the studied nucleotide analogs (AMP.PNP, ATPγS, $ADPBeF_x$, $ADPV_i$), which occupy the γ-phosphate site in the nucleotide-binding pocket, generated the same fluorescence spectra as MgATP with M_{W239+}. This indicates that the fluorescence of W239 is not sensitive to the open–closed transition of switch 2 in different nucleotide-bound forms (Malnasi-Csizmadia *et al*, 2001). In summary, the large fluorescence change of M_{W239+} and M_{W242+} upon adding nucleotides offered good experimental systems for investigations of switch 1 movements.

Nucleotide-binding kinetics of M_{W239+} and M_{W242+}

The large nucleotide-induced intrinsic fluorescence quench allows us to follow the kinetics of nucleotide binding using a stopped-flow device. At 20°C, the signal change of W239 induced by mixing the construct with MgATP or MgADP under pseudo-first-order conditions could be fitted with a single exponential function. From the concentration dependence of the observed rate constant, both the MgATP and MgADP binding of M_{W239+} follow two-step binding kinetics indicative of an induced-fit mechanism (see kinetic data in Supplementary Table SI).

Nevertheless, at 5 and 12°C, the records for M_{W239+} upon MgADP binding show intriguing features. The fast quenching phase corresponding to the MgADP binding was followed by a slower enhancement phase, with rate constants of $k_{iso,observed} = 32$ and 55 s^{-1} at 5 and 12°C, respectively (Figure 2; Supplementary Table SI). This slower phase indicates a novel equilibration step after the binding step. Interestingly, this conformational equilibrium appears to be associated only with the middle of the switch 1 loop, because this transition was not detected in M_{W242+}, as it showed simple two-step binding kinetics for ATP and ADP (see Supplementary Table SI).

The two MgADP states in M_{W239+} are denoted as †M.ADP and *M.ADP for the quenched and enhanced states, respectively. Note that these differ from the nomenclature used previously for different switch 2 states, that is $M^{\dagger}$.Nu and M*.Nu (where Nu refers to a bound nucleotide) (Malnasi-Csizmadia *et al*, 2000).

We further investigated the possible equilibrium of ADP states sensed by W239 using temperature and pressure perturbations.

Characterization of the isomerisation of myosin–MgADP complex

The temperature dependence of the steady-state fluorescence intensity of M_{W239+} was monitored in the absence and presence of different nucleotides. Figure 3 shows that the temperature dependencies of the fluorescence of apo, MgATP and MgAMP.PNP forms are very similar. In contrast, the

temperature dependence of the fluorescence differs when M_{W239+} was complexed with MgADP above 8°C, whereas at lower temperatures, its fluorescence was similar to that of the ATP form. This indicates that M_{W239+}.MgADP complex exists in at least two states in equilibrium above 8°C. This agrees with the observation at 5°C, where the fluorescence spectrum of M_{W239+}.MgADP complex is the same as that in the presence of MgATP and MgAMP.PNP. A multiple ATPase turnover experiment carried out at 5°C also confirmed this finding (see Supplementary data). These data indicate that the low-fluorescence MgADP state (†M) has the same state of switch 1 as the MgATP-bound form. However, the fluorescence level of *M state cannot be uniquely determined from these experiments because of its fractional occupancy at all accessible temperatures. Nevertheless, the results indicate that the two MgADP states are in equilibrium at room temperature and are perturbable by temperature. In the case of M_{W242+} the temperature dependence of the MgADP-bound form was identical to the other forms (apo, MgATP, MgAMP.PNP), and hence only one MgADP state was detected (data not shown).

As the equilibrium of †M.MgADP and *M.MgADP is temperature dependent, a temperature-jump experiment is appropriate to characterize this transition. Figure 4A shows temperature-jump records of M_{W239+} in the presence of saturating MgADP or MgAMP.PNP. In the presence of MgADP a relatively large fluorescence increase 4.7% occurs with a rate constant of 70 s^{-1} induced by a 6°C temperature jump to 20°C. In the apo and rigor states and in the presence of MgAMP.PNP and Mg^{2+}-free ADP (i.e. in the presence of 5 mM EDTA), no significant fluorescence change was detected. Actin also locks the M_{W239+}.MgADP complex into a single state because no transition was detected in the presence of actin at saturating concentration of MgADP (see Supplementary Figure S3).

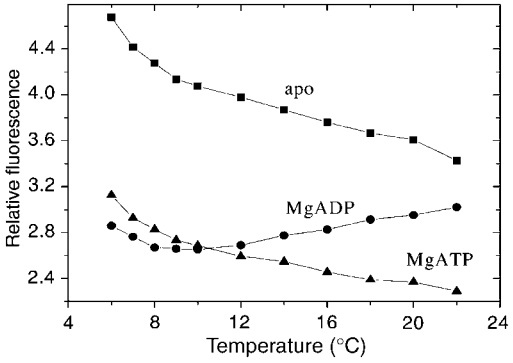

Figure 3 Temperature dependence of M_{W239+} (3 μM) fluorescence in the absence of nucleotide (■) and in the presence of MgATP (1 mM) (▲) and MgADP (1 mM) (●). At low temperature, the fluorescence intensities in the presence of MgATP were slightly higher than those in the presence MgADP; however, in ATP turnover experiments, a fluorescence intensity change cannot be detected after ATP consumption. Fluorescence intensities in the presence of MgATP and MgAMP.PNP were identical at all temperatures.

Pressure-jump experiments confirmed these findings (Figure 4B). A similar fluorescence transition of M_{W239+}.MgADP complex was detected, which was absent in all of the other conditions studied (MgAMP.PNP, ADP + EDTA, actin, actin + MgADP). Note that the pressure-jump records of M_{W239+}.MgADP had two phases. At 20°C, the fast phase was 143 s^{-1} and the slow phase was 29 s^{-1}. A careful evaluation of temperature-jump records confirmed this finding. However, it is difficult resolve the phases because of the lower signal to noise ratio of the latter method. In the pressure-jump experiments in the case of apo, MgAMP.PNP, Mg^{2+}-free ADP, rigor and acto-M_{W239+}.MgADP states, extremely fast (>2500 s^{-1}) phases were found. These extremely fast phases are probably not related with the isomerization found in the presence of MgADP. Further investigations are required to characterize these fast transitions.

In summary, temperature-jump and pressure-jump experiments demonstrate that there are at least two MgADP states in equilibrium, whereas the absence of Mg^{2+}, presence of actin or γ-phosphate site occupation locks the system into a single state with respect to the environment around W239.

Mg^{2+} binding to M_{W239+}.ADP and determination of the equilibrium constant of myosin-MgADP states

Previous studies showed that Mg^{2+} and nucleotide binding and dissociation are related processes (Bagshaw *et al*, 1974; Hannemann *et al*, 2005; Rosenfeld *et al*, 2005). We compared the fluorescence intensity of apo M_{W239+} and its complexes with ADP, AMP.PNP, ATP and actin in the presence and absence of Mg^{2+}. We found that removing Mg^{2+} from M_{W239+} caused a significant fluorescence change only in the presence of ADP and absence of actin. Therefore, we explored the mechanism of Mg^{2+}-free ADP binding to M_{W239+} and Mg^{2+} binding to M_{W239+}.ADP.

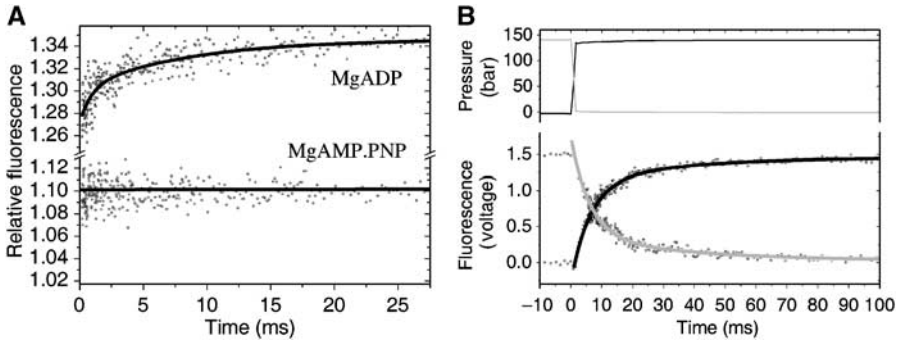

Figure 4 Temperature-jump (**A**) and pressure-jump (**B**) rapid perturbation experiments with M_{W239+} in the presence of MgADP (A, B) and AMP.PNP (A) at 20°C. Tryptophan fluorescence was followed within 100 μs of a 6°C temperature jump (A) and 150 bar pressure jump (B) (see Materials and methods). Pressure increase: black lines; pressure decrease: gray lines.

The addition of ADP to M_{W239+} in the absence of Mg^{2+} gave a 45% quench in tryptophan fluorescence (cf. the fluorescence quench was 20% in the presence of Mg^{2+}). Stopped-flow measurements showed that Mg^{2+}-free ADP equilibrium dissociation constant is similar to that of MgADP; however, the binding and dissociation of the former are faster (see kinetic data in Supplementary Table SI). The Mg^{2+}-free M_{W239+} ADP complex is likely to be a single state because neither temperature nor pressure perturbed the fluorescence. This fluorescent state is different from the ATP-bound state (†M in Scheme 1) because the emission maximum is 9 nm red-shifted (349 nm) compared which that of the †M state (340 nm).

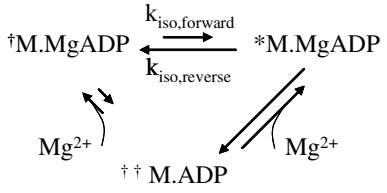

Scheme 1

When Mg^{2+} was removed quickly from the M_{W239+}.MgADP complex by rapid mixing with excess EDTA, the fluorescence intensity dropped in two phases (Figure 5). The observed rate constants of the two phases were 89 and 18 s^{-1} at 11°C. The concentration of ADP was 1 mM in both syringes to ensure that the M_{W239+} was saturated with ADP throughout.

When a saturating concentration of Mg^{2+} (5 mM) was mixed rapidly with M_{W239+}ADP, the profile of the fluorescence record was dramatically different from that of the Mg^{2+} dissociation from M_{W239+}.MgADP: a rapid enhancement phase (120 s^{-1}) was followed by a slow quench phase (20 s^{-1}) at 11°C (Figure 5). According to these data, a two-step Mg^{2+}-binding model is required, in which Mg^{2+} exchange occurs predominantly with the *M state and the slow phase represents the equilibration of *M and †M states (Scheme 1 (complete thermodynamic box of Scheme 1 in Supplementary data)). The rate constants of the quenching phase at different temperatures were in line with the rate constants calculated from the temperature-jump and the pressure-jump experiments.

Because the fast Mg^{2+} binding phase is significantly faster than the quenching phase, the extrapolated end point of the enhancement phase determines the fluorescence intensity of the *M state (see its value below). The fluorescence level of the Mg^{2+}-free ††M state relative to the †M state fluorescence is known from the spectra of Mg^{2+}-free ADP complex and ATP (or AMP.PNP). Consequently, the equilibrium constants of the isomerization between the *M and †M MgADP forms can be determined from the relative fluorescence intensities of the end points of the records measured at different temperatures. We applied a global fit method (Berkeley Madonna software) to these experimental data using the binding mechanism described in Scheme 1 to deduce the elementary rate constants (Table I) and the precise values of the relative fluorescence intensities of the states. The relative intensities of *M and †M states are 1.13 and 0.63, respectively, taking the apo state as unity. Similar values for the elementary constants were obtained

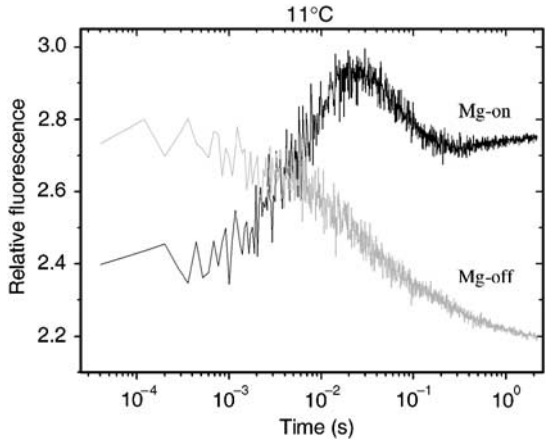

Figure 5 Stopped-flow records on Mg^{2+} dissociation from the M.MgADP complex and Mg^{2+} binding to the M.ADP complex monitored by tryptophan fluorescence at 11°C. Mg-off: 2 μM M_{W239+} and 1 mM ADP were mixed with 5 mM EDTA and 1 mM ADP in the conventional buffer (see Materials and methods). Mg-on: Mg^{2+} binding to the ADP complex of M_{W239+}.2 μM M_{W239+}, 1 mM ADP and 3 mM EDTA were mixed with 10 mM $MgCl_2$ and 1 mM ADP in the conventional buffer. The increasing phase and quenching phase of the record represent Mg^{2+} binding and the equilibration of the two MgADP states, respectively. Rate constants were determined by simulation of a three-step mechanism (Scheme 1) using Berkeley Madonna software and summarized in Table I. In the simulation, we used a temperature series of Mg^{2+}-binding and Mg^{2+}-dissociation stopped-flow experiments. Simulations of both experiments gave the consistent result that the main flux of Mg^{2+}-binding and -dissociation reaction occurs through the high-fluorescence MgADP-myosin state.

when stopped-flow records of MgADP binding experiments (Figure 2) were fitted (Table I). The equilibrium constant of $K_{iso} = [*M]/[^{\dagger}M]$ equilibrium is 0.7 at 20°C and the calculated thermodynamic parameters are: $\Delta G_0 = 0.9$, $\Delta H_0 = 44$ kJ/mol and $\Delta S_0 = 0.15$ kJ/mol K. These results are consistent with the results of the temperature dependence of fluorescence intensities of AMP.PNP (†M state) and MgADP (mixture of †M and *M) complexes (Figure 3). That experiment also shows that below 8°C, the fluorescence intensity of the M_{W239+}.MgADP complex reaches the fluorescence of the †M state because the lower the temperature, the smaller the equilibrium constant of $K_{iso} = [*M]/[^{\dagger}M]$.

The mechanism of MgADP binding to M_{W239+}

The results of stopped-flow experiments of MgADP binding (Figure 2) are consistent with the calculated rate constant values obtained from the Mg^{2+} association and dissociation experiments (Figure 5) as presented above. A general mechanism for MgADP binding to M_{W239+} is summarized in Scheme 2 (see complete thermodynamic box of Scheme 2 in Supplementary data).

In this scheme, both the †M and *M states are capable of binding MgADP, but under some conditions, the flux through one route may dominate. At high temperature, MgADP binding stopped-flow records have a single phase, but at 5 and 12°C, the rapid quenching phase is followed by a small increasing phase (Figure 2). The relative equilibrium constants of the †M and *M states for MgADP binding are determined by the equilibrium constant of the *M to †M transition because these states form a thermodynamic box. At low temperature, the predominant form of M.MgADP

Table I Elementary rate constants of the equilibrium of $^{\dagger}M_{W239+}$.MgADP and $^{*}M_{W239+}$.MgADP states

Rate constant	Data analyzed	20°C	12°C	5°C
$k_{iso,\ forward}$ (s^{-1})	Mg^{2+} binding/dissociation	20	6	≈1
$k_{iso,\ backward}$ (s^{-1})		29	18	12
K_{iso}		0.7	0.3	≈0.1
$k_{iso,\ forward}$ (s^{-1})	MgADP binding	—	23	3
$k_{iso,\ backward}$ (s^{-1})		—	32	29
k_{1on} ($\mu M^{-1} s^{-1}$)		3.8	3.5	3.3
k_{2on} ($\mu M^{-1} s^{-1}$)		2.7	0.57	≈0.15

Global fit analysis of experimental data was used to determine the rate constants (see Figures 2 and 5) by applying the binding mechanisms described in Schemes 1 and 2. In order to determine the relative fluorescence intensities of *M, M_{apo} and $^{\dagger}M$, the records of Mg^{2+} binding and dissociation from stopped-flow experiments at different temperatures were fitted separately. The individual rate constants and the fluorescence level of *M were left as free parameters, but we fixed the values of the relative intensities of the $^{\dagger}M$ and $^{\dagger\dagger}M$.ADP (Mg^{2+}-free) forms. We consider that the Mg^{2+} exchange of $^{\dagger}M$ is relatively low (see Scheme 1). From the relative intensity of *M to $^{\dagger}M$, the relative fluorescence of apo state to $^{\dagger}M$ and *M can be determined: the relative intensities of *M and $^{\dagger}M$ states are 1.13 and 0.63, respectively, taking the apo state as unity. This global fit analysis also determines the elementary rate constants of the equilibrium of $^{\dagger}M_{W239+}$.MgADP and $^{*}M_{W239+}$.MgADP states (Table I). By applying the relative fluorescence intensity values of *M and $^{\dagger}M$ states determined in the global fitting described above, the elementary rate constants of Scheme 2 can be calculated from the MgADP binding in stopped-flow experiments by using global fit analysis. In the analysis, the equilibrium constant of the *M/$^{\dagger}M$ equilibrium was fixed to the value determined from the Mg^{2+}-binding and dissociation experiments.

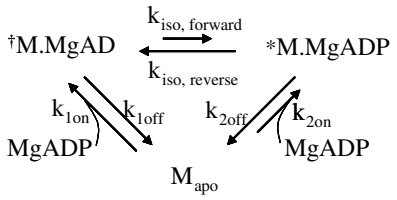

Scheme 2

is $^{\dagger}M$; therefore the affinity of MgADP to $^{\dagger}M$ is higher than that to *M. The relative population of *M increases with increasing temperature. At 12°C, $^{\dagger}M$.MgADP binding is still dominant, but the subsequent isomerization to *M.MgADP now gives the slower enhancement phase with a larger amplitude. However, at higher temperatures (e.g. 20°C), this second phase is lost, indicating that MgADP now binds directly to the *M state. Scheme 2 might be made more general by considering the M_{apo} state to be an equilibrium mixture of $^{\dagger}M$ and *M to give an intermediate fluorescence level. However, this is inconsistent with the lack of perturbation of the putative equilibrium by temperature (see temperature- and pressure-jump experiments in Figure 4). This suggests that the W239 residue of the apo state is in a different environment to either $^{\dagger}M$ or *M.

Actin induced fluorescence change of M_{W239+} and M_{W242+}

An important question is whether actin binding induces a change in the switch 1 region as implied from structural data (Coureux *et al*, 2003, 2004). To test this hypothesis, actin was mixed with M_{W239+} under different conditions in stopped-flow, and the fluorescence change of W239 tryptophan was followed in parallel with the light scattering change. We were careful to avoid stray light and auto-fluorescence of the emission filter by using a selected interference filter (see Materials and methods) because during the actomyosin association, light scattering of the solution can give an artifactual signal in the fluorescence channel (Conibear *et al*, 2004).

When M_{W239+} and actin were mixed in stopped-flow, a 4.3% increase in protein fluorescence was observed, which paralleled the light scattering profile. This corresponds to an approximately 15% fluorescence change relative to the fluorescence of W239, assuming there is no change in actin fluorescence or light scattering artifact. This change is similar to the difference in fluorescence intensities of the *M state and apo state. The actin-induced fluorescence change of the M_{W242+} construct was less than 1.5%. These results indicate that the conformation of the switch 1 loop or the environment of W239 changes upon actin binding.

In order to characterize how actin binding and switch 1 movement are coupled, we studied the ATP- and ATPγS-induced actin dissociation reactions. Acto-M_{W239+} was mixed with ATP under pseudo-first-order conditions. The rate constant of ATP binding to the myosin motor domain as determined from the tryptophan fluorescence change was slower in the presence of actin than in its absence (Conibear *et al*, 2004). The rate constants for tryptophan fluorescence change were similar to those deduced from the light scattering change. However, the fluorescence signal always slightly preceded the light scattering signal change. A similar effect was observed when a fluorescent probe was located in the actin-binding cleft of myosin (Conibear *et al*, 2003). The expected lag phase of the light scattering signal is difficult to detect because of the fast actin dissociation and the low signal-to-noise ratio at the beginning of the records.

As actin dissociation is slow in the presence of ATPγS, it is a potentially useful substrate analog to study the coupling of actin dissociation and switch 1 movement (Conibear *et al*, 2003; Malnasi-Csizmadia *et al*, 2005). Acto-M_{W239+} was mixed with 100 μM ATPγS and tryptophan fluorescence was measured in parallel with light scattering (Figure 6). The triphasic fluorescence change yielded rate constants of $k_{obs,fluor1} = 68\ s^{-1}$, $k_{obs,fluor2} = 4.3\ s^{-1}$, $k_{obs,fluor3} = 0.10\ s^{-1}$ (relative amplitudes: $A_{fluor1} = 0.53$, $A_{fluor2} = 0.14$, $A_{fluor3} = 0.33$), with the slow phases corresponding to the two phases of the light scattering change ($k_{obs,light\text{-}scat1} = 4.2\ s^{-1}$, $k_{obs,light\text{-}scat2} = 0.11\ s^{-1}$; relative amplitudes: $A_{light\text{-}scat1} = 0.25$, $A_{light\text{-}scat2} = 0.75$). The light scattering change is also similar to previous measurements of the ATPγS-induced dissociation rate constant for myosin using pyrene-actin as a probe (Malnasi-Csizmadia *et al*, 2005). The fast phase of the

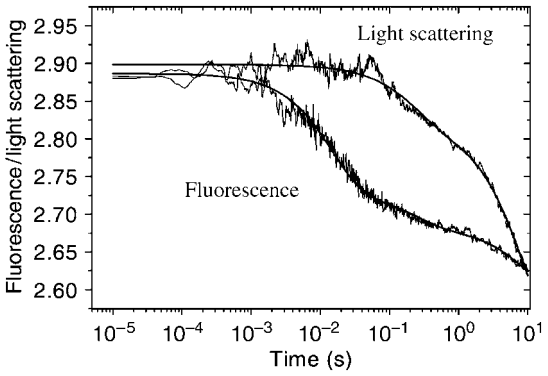

Figure 6 Time course of the fluorescence intensity and light scattering signal for the reaction of 2 μM M_{W239+} with 100 μM of MgATPγS in the stopped-flow apparatus at 20°C. The light scattering record is normalized to the fluorescence record for better visual comparison. The light scattering signal follows the progress of actomyosin dissociation and was fitted with double exponential ($k_{obs,light\text{-}scat1} = 4.2\ s^{-1}$, $k_{obs,light\text{-}scat2} = 0.11\ s^{-1}$). The fluorescence change record was fitted with triple exponential ($k_{obs,fluor1} = 68\ s^{-1}$, $k_{obs,fluor2} = 4.3\ s^{-1}$, $k_{obs,fluor3} = 0.10\ s^{-1}$). During the fastest phase of fluorescence change, the extent of actomyosin dissociation is limited. As the fastest phase of the fluorescence change precedes the light scattering change, it shows that conformational rearrangement in switch 1 is followed by actin dissociation.

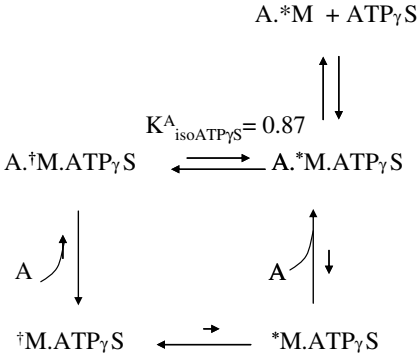

Scheme 3

fluorescence signal change was 53% of the total change. These results indicate that a conformational change in switch 1 could initiate actin dissociation, but these movements do not occur in synchrony, as might be expected for rigid-body coupling via the upper 50 K domain. A model is shown in Scheme 3 in which acto-*M.ATPγS and acto-†M.ATPγS equilibrate before significant actin dissociation occurs. As this equilibrium is much faster than the actin dissociation steps, the fluorescence levels at the start and the end represent the *M and †M populations, respectively, and the relative amplitudes of the phases of the fluorescence signal change determine the equilibrium constant, $K^{A}_{iso\text{-}ATP\gamma S} = [A.{*}M.ATP\gamma S]/[A.{\dagger}M.ATP\gamma S] = (A_{fluor\ 2} + A_{fluor\ 3})/A_{fluor\ 1} = 0.87$.

Relations of fluorescence and enzymatic states of M_{W239+}

Figure 7 shows stopped-flow records, which allow comparison of the amplitudes of the actin-induced fluorescence intensity changes of M_{W239+} in the presence and absence of MgADP and the amplitudes of nucleotide-induced fluorescence signal changes of M_{W239+} in the presence and absence of actin. The fluorescence intensity of actin is subtracted from the records where actin was present. We found that at 20°C, the amplitude of the actin-induced fluorescence change was much higher in the presence of MgADP than in its absence; however, the observed rate constants were similar. There was no significant fluorescence change when actoM_{W239+} was mixed with MgADP, and the actin dissociation was less than 10% based on the light scattering signal. At 20°C, MgADP binding is fast and its signal change was lost in dead time so that the horizontal record shows the end-point fluorescence intensity of the M_{W239+}.MgADP complex. The fluorescence level at the end of the reaction represents a mixture of *M and †M populations in equilibrium. Altogether, the results suggest that the W239 residue in switch 1 in acto-M_{W239+}.MgADP is in the same environment as in the rigor state, and is distinctly different from that in the apo M_{W239+} state. Consequently, in the presence of Mg^{2+}, three structural states can be distinguished: †M, *M and apo. Myosin complexed with MgATP or substrate analogs having γ-phosphate and low-fluorescence MgADP states represent the †M state. Rigor, MgADP high-fluorescence state and acto-M.MgADP ternary complex represent the *M state.

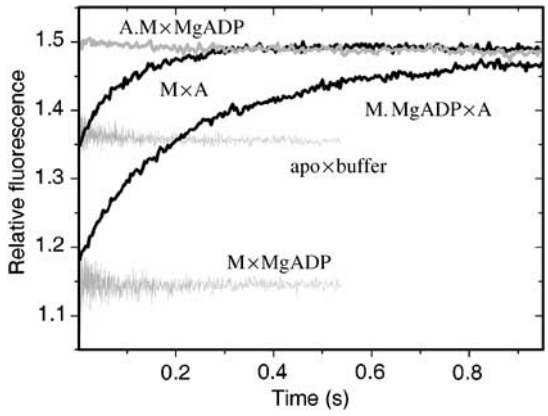

Figure 7 Stopped-flow records of the reactions of M_{W239+} with actin in the presence (black, M.MgADP × A) and absence (black, M × A) of MgADP, the reaction of acto-M_{W239+} with MgADP (gray, A.M × MgADP) and M_{W239+} with MgADP (gray, M × MgADP). The control experiment was when M_{W239+} was mixed with assay buffer (gray, apo × buffer). The fluorescence intensity of actin was substracted from records of the experiments in which actin was present. The M_{W239+} concentration was 2 μM, MgADP 1 mM and actin was stoichiometric to M_{W239+}. All the reactions were carried out at 20°C. The experiments in the absence of actin were recorded in log time-base and oversampling. In the record of the reaction of M_{W239+} mixed with 1 mM MgADP (gray, M × MgADP), the fast quenching phase occurred in the dead time of the stopped flow (see Figure 2).

Discussion

Based on structural data, the switch 1 loop of myosin is presumed to play a central role in information transmission between the nucleotide- and the actin-binding regions. Recent structural data show that switch 1 can exist in different conformational states. Solution experiments are now required to explore the role of switch 1 and to elucidate the mechanism of its action; therefore, we have investigated the movement of switch 1 upon nucleotide and actin binding.

In a broader context, switch 1 is of interest because it is a common structural element in the family of P-loop NTPases (Kull *et al*, 1998), and its members (G-proteins, myosin and kinesin) may share an analogous mechanism (Klebe *et al*, 1995; Goody and Hofmann-Goody, 2002). The nucleotide exchange in these systems occurs in similar ways: G-proteins and their GEFs are analog proteins of the motor enzymes (myosin or kinesin) and the partners protein (actin or tubulin), respectively. These data provide a good basis for the comparison of the detailed mechanisms of nucleotide exchange in G-proteins and myosin.

Tryptophans F239W and F242W were introduced into the switch 1 region of *Dd* myosin II motor domain, whereas native tryptophans were substituted with phenylalanine residues to reduce background fluorescence. These single fluorophores provide specific signals for conformational changes of switch 1 during the ATPase cycle of actomyosin, nucleotide binding and actin interaction of the motor domain. The MgADP equilibrium binding constants are practically unchanged for M_{W239+}; however, MgADP binding (and dissociation) of M_{W239+} was slightly faster ($6.5 \times 10^6\,M^{-1}\,s^{-1}$ for M_{W239+}, $1.4 \times 10^6\,M^{-1}\,s^{-1}$ for wild type; Malnasi-Csizmadia *et al*, 2000). Also actin binding into the ternary acto-M.MgADP complex is slightly stronger (0.04 μM) than was the case with the wild type construct (0.12 μM); however, the rigor complexes are similar to each other (0.03 μM). The main perturbation caused by F239W mutation is the large reduction in the rate constant of the hydrolysis step, which becomes the rate-limiting step. Consequently, the ATPase activation by actin is also limited in M_{W239+} (for further details see Supplementary data). However, hydrolysis is not directly coupled to the interactions of actin and myosin (Conibear *et al*, 2004); so these constructs are suitable preparations for investigations of the relationship between switch 1 movements and actin binding.

Three fluorescent states of W239 were distinguished in the presence of Mg^{2+} and a fourth state is the Mg^{2+}-free ADP state (Table II). In the presence of MgADP, two states are in equilibrium. One of these states (†M) in the presence of MgADP could be the same state as the ATP state and the other state (*M) is different from the myosin apo state. Actin also induces a structural change in switch 1. As the fluorescence level of the acto.M rigor complex is the same as *M in the presence of MgADP and MgADP does not induce a fluorescence change in acto-M_{W239+}, the rigor complex could have the same switch 1 state as the acto-M_{W239+}.MgADP ternary complex and *M states.

In G-proteins, single trypthophans have also been introduced into the switch 1 loop. Y32W (Rensland *et al*, 1995) and Y40W (Yamasaki *et al*, 1994) mutants were produced in p21 ras, which are homolog positions to the N234 and F242 in *Dd* myosin II, respectively. Interestingly, a similar tendency can be seen in the fluorescence levels complexed with different nucleotide with p21 ras to our constructs. The Y32W construct shows large fluorescence intensity difference in the presence of GDP and GTP, or its analog, as in the case of M_{W239+} constructs with ADP and ATP. However, only a very small difference can be detected in the fluorescence of Y40W GDP and GTP analog complexes, as we found with the M_{W242+} construct. Unfortunately, no experimental data are available as to whether Y32W or Y40W p21 ras constructs show fluorescence changes upon binding to GEF proteins. Nevertheless, based on fluorescence (Rensland *et al*, 1995; Diaz *et al*, 1997; Kuppens *et al*, 2003) and NMR (Yamasaki *et al*, 1994) studies on p21 ras in the presence of nucleotides, two states can be distinguished. Nucleotide binding and GEF binding are strongly negatively coupled and the coupling with GTP is not very different from GDP (Goody and Hofmann-Goody, 2002; Itzen *et al*, 2006).

The *Dd* myosin II motor domain switch 1 exists in two states with MgADP and the two states bind MgADP differently. The relative binding constants and the rate constants define the fluxes of MgADP binding of †M and *M. As MgADP binding and the equilibrium of MgADP complexes of †M and *M form a thermodynamic triangle, the latter equilibrium defines the ratio of the MgADP binding constants. This equilibrium is highly temperature-sensitive and at low temperature, the predominant form is †M; therefore this state binds MgADP much tighter than *M. At room temperature, the ratio of †M.MgADP to *M.MgADP is 2:1; consequently, the ratio of the binding constants becomes smaller. Nevertheless, we can define †M as a strong MgADP-bound form, whereas *M is the weak MgADP-bound form. Mg^{2+} binding of the two forms of ADP complex is also different. Mg^{2+} exchange occurs practically via *M state, whereas †M.Mg.ADP is formed and looses Mg^{2+} through the *M.Mg.ADP form (Scheme 1). Using a structure-specific signal, our Mg^{2+} and ADP binding model is in line with the models described by Rosenfeld *et al* (2005) and Hannemann *et al* (2005) in which they proposed a two-ADP-state model, based on mant-ADP binding kinetics to myosin V. In contrast to their model, we propose that for *Dd* myosin II motor domain, only one of the states exchanges Mg^{2+}, but both exchange MgADP at room temperature. It is contro-

Table II Summary of the relationship of the fluorescence intensity levels of W239, the nucleotide states and the structural states

Relative fluorescence intensities of W239	Ligands bound to myosin	Structural states	Nomenclature
High fluorescence (*M): 113% (360 nm)[a]	Actin and/or MgADP	1W7I	– Weak ADP-bound state – Open switch 1
Intermediate fluorescence (M): 100% (350 nm)	None (Apo state)	1W8J, 1Q5G	Apo
Low fluorescence (†M): 63% (340 nm)	– Nucleotides or analog in which the γ-phosphate site is occupied (ATP, ADP.P_i, AMP.PNP) – MgADP	1W7J, 1MMA, 1MMD, 1MMG, 1MMN, 1MND, 1MNE, 1VOM	Closed switch 1
Lowest fluorescence (††M): 55% (349 nm)	Mg^{2+}-free ADP		

[a]Emission peak wavelength is calculated from relative intensities and the detected peak wavelength shifts of the states.

versial whether the Mg^{2+}-free state is predominantly a single state, as Hannemann *et al* (2005) suggest, or remains a two-state equilibrium, as proposed by Rosenfeld *et al* (2005). Our results suggest that the Mg^{2+}-free ADP state is a single state of switch 1 region, which is different from both MgADP states. The difference between these results could reflect differences between myosin II and myosin V, or be a consequence of the structure-specific probe used in our studies compared with the mant-ADP used in the studies cited above.

The equilibrium between †M and *M is strongly affected by actin and ATP. ATP and analogs with a γ-P_i group push the equilibrium towards the †M state, whereas actin, either in the presence or absence of MgADP, pushes it towards the *M conformation of switch 1. This finding is similar to the Hannemann *et al* (2005) model for myosin V in which the isomerization of the MgADP states is pushed predominantly to a single state; however, Rosenfeld *et al* (2005) did not find this effect with myosin V. Two ADP states of actomyosin II have been supposed for many years and is key to the load-dependent ADP release in muscle (Sleep and Hutton, 1980; Cremo and Geeves, 1998; Coluccio and Geeves, 1999). Strain-dependent ADP release also plays an important role in the mechanism of processivity of myosin V (Veigel *et al*, 2005). One of the MgADP states is favored when mechanical strain is developed in the head by an internal load (Rosenfeld and Sweeney, 2004).

*Structural implications of †M, *M and apo states in myosin*

Before the determination of the structure of apo state of *Dd* myosin II motor domain (Reubold *et al*, 2003), all of the *Dd* myosin motor atomic structures showed switch 1 in the closed state. The *Dd* myosin II motor domain structure of Reubold *et al* (2003) was significant because switch 1 was proposed to be in an open state in the absence of nucleotide. Coureux *et al* (2004) published myosin V structures in which the switch 1 loop was in an open state in the apo and MgADP-bound forms. They also found that the structures with an open switch 1 had a closed actin-binding cleft. It was proposed that switch 1 closure opens the actin binding-cleft and vice versa, which results in weak and strong actin-binding states, respectively (Holmes and Schroder, 2003). Nevertheless, our results with ATPγS show that switch 1 closure does not occur at the same time as actin-dissociation. Consequently, switch 1 loop and actin binding cleft do not move together as a rigid body, but the open–closed equilibrium between the states in one of the regions is coupled to the closed–open equilibrium of the other region.

There is evidence for two structural states of switch 1 in the presence of MgADP (1W7I and 1MMA). Coureux *et al* (2004) suggested that in the ADP form with open switch 1 (termed *weak ADP-bound state*), Mg^{2+} and ADP are bound more weakly than in the state with a closed switch 1. We found that the high-fluorescence *M state binds MgADP more weakly than †M, especially at low temperature. We suggest that the *M state can be assigned to the switch 1 open structural state (turned *weak ADP-bound state*), whereas the †M is the switch 1 closed form. Coureux *et al* (2004) found switch 1 in the same position in the weak ADP-bound and apo (rigor-like) states, whereas the P-loop is positioned slightly differently. This structural difference might explain the small difference in the fluorescence of *M and apo states.

Strong and weak actin binding according to the nucleotide binding states

The strength of actomyosin binding depends on the nature of the bound nucleotide. ATP and ATP-like nucleotide analogs result in weak actomyosin complexes, whereas the ADP-bound form results in a strong binding complex. It is supposed, based on structural information, that the switch 1 open state binds actin much tighter than the closed form (Holmes *et al*, 2003; Reubold *et al*, 2003). For illustration, we suppose that the strong binding state has a K_d of about 0.1 μM (based on the actin affinity for M.ADP), whereas the weak binding state has a K_d of about 50 μM (estimated from the K_M of the ATPase for actin, which might be a slight underestimation of K_d). We show here that actin pushes the equilibrium of the switch 1 states towards the open (*M) state. A thermodynamic box of these events (Scheme 4A) indicates that the dominant state of the four states is the actomyosin switch 1 open form ($A._oM.ADP_{Mg}$).

The scheme is consistent with the fact that MgADP–myosin complex binds actin strongly. In contrast, in the presence of ATP (or other nucleotide analogs in which γ-phosphate site is occupied with phosphate or analogs), the equilibrium of the switch 1 states is pushed strongly towards the closed (†M) form. Also, we found that the two states of switch 1 are in equilibrium ($K^{A}_{iso\text{-}ATP\gamma S} = 0.87$) in the ternary complex in the presence of ATPγS. What happens in the thermodynamic box if ATP or an ATP analog is bound? We assume that actin binding is dependent only on the state of switch 1 and not directly on the nature of the bound nucleo-

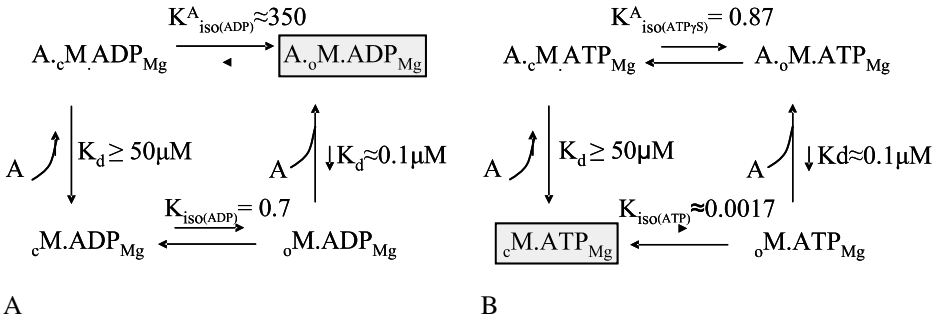

Scheme 4

tide. The consequence is that the predominant state of this thermodynamic box is the actin-free switch 1 closed myosin state ($_cM.ATP_{Mg}$), which correlates with the fact that a weak actomyosin complex is formed in the presence of ATP and ADP.P_i (Scheme 4B). The conclusion is that the strength of actin binding to myosin is highly sensitive to the equilibrium constant of the switch 1 open–closed equilibrium. Consequently, the nature of the bound nucleotide, especially the occupation of the γ-phosphate site, adjusts the equilibrium of switch 1 open and closed states, which controls the actomyosin interaction.

This model is an extension of the model of nucleotide exchange in P-loop NTPases as described by Goody and Hofmann-Goody (2002). They compared the kinetics of nucleotide exchanges in G-proteins, myosins and kinesins. They pointed out that nucleotide exchange occurs by negative coupling between the binding of exchange factor and the nucleotides in an allosteric way. Here, we extend this model with a specific structural element (switch 1) having two states (at least) where the equilibrium constant between these states of switch 1 determines the coupling ratio of nucleotide and exchange factor binding constants. As we discussed above, this model is probably also valid for G-proteins; however, further experiments are required to establish this.

Materials and methods

Protein engineering, expression and purification

W239F or W242F were introduced into the tryptophan-less *Dd* M761 motor domain cDNA fragment, and the mutant recombinant proteins were expressed in *Dd* AX2-ORF+ cells and isolated by using His-tagged affinity chromatography as described previously (Malnasi-Csizmadia *et al*, 2000). The motor domain preparation so obtained was dialyzed against an assay buffer containing 40 mM NaCl, 20 mM HEPES pH 7.5, 1 mM $MgCl_2$ and 2 mM mercaptoethanol. All experiments were performed in this buffer, unless otherwise indicated.

Fluorescence measurements

Steady-state measurements were carried out with Spex320 Fluoromax fluorimeter equipped with 150 W Xe lamp using 10 mm pathlength cell. Tryptophan was excited at 296 nm using 2-nm excitation and emission slits. The temperature dependence of the fluorescence detected at 345 nm was measured by heating the sample from 6 to 26°C and the recorded fluorescence intensities were assigned to discrete temperature values.

Transient kinetics

Stopped-flow experiments were conducted using a KinTek SF-2004 Stopped-Flow fluorimeter (KinTek Corporation, USA) equipped with a 150 W Hg–Xe Super-quiet lamp (Hamamatsu Photonics, Enfield, UK). Tryptophan was excited at 297 nm; the slit was 4 nm. The detection setup of the tryptophan fluorescence was improved by using a 340-nm interference filter (bandwidth: 10 nm) (Corion CFS-001999 9L134) in the emission channel rather than a WG335 cutoff filter and UG11 bandpass filter combination. The interference filter showed a hundred times less UV-induced fluorescence, and the sum of the intensity of fluorescence and transmitted light at 297 nm was much smaller than the filter combination. The interference filter allowed small changes in tryptophan fluorescence to be measured in reactions accompanied by significant changes in light scattering during actomyosin complex formation and dissociation. The different profiles of the light scattering and fluorescence records measured in parallel (e.g. Figure 6) proved that light scattering did not dominate the fluorescence measurement. Light scattering was recorded simultaneously with a second photomultiplier, where no filter was used. The dead time of the instrument was determined as 1.5 ms at the flow rate of 14 ml/s. The transients were analyzed by Origin 7.5 (OriginLab). Temperature-jump experiments were carried out with a TJ-64 System (Hi-Tech Scientific, Salisbury, UK) as described previously (Malnasi-Csizmadia *et al*, 2001), but the emitted light was measured through the 340-nm interference filter. Pressure-jump experiments were performed on a custom-built apparatus (Pearson *et al*, 2002). Each measurement was the result of at least 500 repeats. Pressure step sizes of 15 MPa were routinely used, as it represented the upper limit to the linear response of amplitude to pressure step size. Tryptophan was excited at 295 nm with a bandwidth of 1.8 nm and emitted light was collected through a WG320 cutoff filter (Schott GmbH, Mainz, Germany).

Supplementary data

Supplementary data are available at *The EMBO Journal* Online (http://www.embojournal.org).

Acknowledgements

We thank Roger Goody for discussions about the nucleotide exchange mechanism of G-proteins. This work was supported by Wellcome Trust IRDA (071525), EMBO YIP, EMBO/HHMI, Bekessy fellowship, National Office for Research and Technology RET 14/2005, OTKA TS49812 to AMC. CRB and WZ acknowledge support from the BBSRC.

References

Bagshaw CR, Eccleston JF, Eckstein F, Goody RS, Gutfreund H, Trentham DR (1974) The magnesium ion-dependent adenosine triphosphatase of myosin. Two-step processes of adenosine triphosphate association and adenosine diphosphate dissociation. *Biochem J* **141:** 351–364

Boriack-Sjodin PA, Margarit SM, Bar-Sagi D, Kuriyan J (1998) The structural basis of the activation of Ras by Sos. *Nature* **394:** 337–343

Coluccio LM, Geeves MA (1999) Transient kinetic analysis of the 130-kDa myosin I (MYR-1 gene product) from rat liver. A myosin I designed for maintenance of tension? *J Biol Chem* **274:** 21575–21580

Conibear PB, Bagshaw CR, Fajer PG, Kovacs M, Malnasi-Csizmadia A (2003) Myosin cleft movement and its coupling to actomyosin dissociation. *Nat Struct Biol* **10:** 831–835

Conibear PB, Malnasi-Csizmadia A, Bagshaw CR (2004) The effect of F-actin on the relay helix position of myosin II, as revealed by tryptophan fluorescence, and its implications for mechanochemical coupling. *Biochemistry* **43:** 15404–15417

Coureux PD, Sweeney HL, Houdusse A (2004) Three myosin V structures delineate essential features of chemo-mechanical transduction. *EMBO J* **23:** 4527–4537

Coureux PD, Wells AL, Menetrey J, Yengo CM, Morris CA, Sweeney HL, Houdusse A (2003) A structural state of the myosin V motor without bound nucleotide. *Nature* **425:** 419–423

Cremo CR, Geeves MA (1998) Interaction of actin and ADP with the head domain of smooth muscle myosin: implications for strain-dependent ADP release in smooth muscle 2. *Biochemistry* **37:** 1969–1978

Diaz JF, Sillen A, Engelborghs Y (1997) Equilibrium and kinetic study of the conformational transition toward the active state of p21Ha-ras, induced by the binding of BeF3- to the GDP-bound state, in the absence of GTPase-activating proteins. *J Biol Chem* **272:** 23138–23143

Goody RS, Hofmann-Goody W (2002) Exchange factors, effectors, GAPs and motor proteins: common thermodynamic and kinetic principles for different functions. *Eur Biophys J* **31:** 268–274

Gulick AM, Bauer CB, Thoden JB, Rayment I (1997) X-ray structures of the MgADP, MgATPgammaS, and MgAMPPNP complexes of the *Dictyostelium discoideum* myosin motor domain. *Biochemistry* **36:** 11619–11628

Hannemann DE, Cao W, Olivares AO, Robblee JP, De La Cruz EM (2005) Magnesium, ADP, and actin binding linkage of myosin V:

evidence for multiple myosin V-ADP and actomyosin V-ADP states. *Biochemistry* **44:** 8826–8840

Holmes KC, Angert I, Kull FJ, Jahn W, Schroder RR (2003) Electron cryo-microscopy shows how strong binding of myosin to actin releases nucleotide. *Nature* **425:** 423–427

Holmes KC, Schroder RR (2003) Switch 1 opens on strong binding to actin. Molecular and cellular aspects of muscle contraction. *Adv Exp Med Biol* **538:** 159–166

Itzen A, Pylypenko O, Goody RS, Alexandrov K, Rak A (2006) Nucleotide exchange via local protein unfolding—structure of Rab8 in complex with MSS4. *EMBO J* **25:** 1445–1455

Klebe C, Prinz H, Wittinghofer A, Goody RS (1995) The kinetic mechanism of Ran—nucleotide exchange catalyzed by RCC1. *Biochemistry* **34:** 12543–12552

Kull FJ, Vale RD, Fletterick RJ (1998) The case for a common ancestor: kinesin and myosin motor proteins and G proteins. *J Muscle Res Cell Motil* **19:** 877–886

Kuppens S, Hellings M, Jordens J, Verheyden S, Engelborghs Y (2003) Conformational states of the switch I region of Ha-ras-p21 in hinge residue mutants studied by fluorescence lifetime and fluorescence anisotropy measurements. *Protein Sci* **12:** 930–938

Malnasi-Csizmadia A, Dickens JL, Zeng W, Bagshaw CR (2005) Switch movements and the myosin crossbridge stroke. *J Muscle Res Cell Motil* **26:** 31–37

Malnasi-Csizmadia A, Pearson DS, Kovacs M, Woolley RJ, Geeves MA, Bagshaw CR (2001) Kinetic resolution of a conformational transition and the ATP hydrolysis step using relaxation methods with a *Dictyostelium* myosin II mutant containing a single tryptophan residue. *Biochemistry* **40:** 12727–12737

Malnasi-Csizmadia A, Woolley RJ, Bagshaw CR (2000) Resolution of conformational states of *Dictyostelium* myosin II motor domain using tryptophan (W501) mutants: implications for the open-closed transition identified by crystallography. *Biochemistry* **39:** 16135–16146

Naber N, Minehardt TJ, Rice S, Chen X, Grammer J, Matuska M, Vale RD, Kollman PA, Car R, Yount RG, Cooke R, Pate E (2003) Closing of the nucleotide pocket of kinesin-family motors upon binding to microtubules. *Science* **300:** 798–801

Pearson DS, Holtermann G, Ellison P, Cremo C, Geeves MA (2002) A novel pressure-jump apparatus for the micro-volume analysis of protein–ligand and protein–protein interactions: its application to nucleotide binding to skeletal-muscle and smooth-muscle myosin subfragment-1. *Biochem J* **366:** 643–651

Rensland H, John J, Linke R, Simon I, Schlichting I, Wittinghofer A, Goody RS (1995) Substrate and product structural requirements for binding of nucleotides to H-ras p21: the mechanism of discrimination between guanosine and adenosine nucleotides. *Biochemistry* **34:** 593–599

Reubold TF, Eschenburg S, Becker A, Kull FJ, Manstein DJ (2003) A structural model for actin-induced nucleotide release in myosin. *Nat Struct Biol* **10:** 826–830

Rosenfeld SS, Houdusse A, Sweeney HL (2005) Magnesium regulates ADP dissociation from myosin V. *J Biol Chem* **280:** 6072–6079

Rosenfeld SS, Sweeney HL (2004) A model of myosin V processivity. *J Biol Chem* **279:** 40100–40111

Sleep JA, Hutton RL (1980) Exchange between inorganic phosphate and adenosine 5′-triphosphate in the medium by actomyosin subfragment 1. *Biochemistry* **19:** 1276–1283

Veigel C, mitz S, Wang F, Sellers JR (2005) Load-dependent kinetics of myosin-V can explain its high processivity. *Nat Cell Biol* **7:** 861–869

Yamasaki K, Shirouzu M, Muto Y, Fujita-Yoshigaki J, Koide H, Ito Y, Kawai G, Hattori S, Yokoyama S, Nishimura S (1994) Site-directed mutagenesis, fluorescence, and two-dimensional NMR studies on microenvironments of effector region aromatic residues of human c-Ha-Ras protein. *Biochemistry* **33:** 65–73

